Original Article

Amelioration of Hypertensive Heart Failure by Amlodipine May Occur *via* Antioxidative Effects

Hiroshi HASEGAWA[1)], Hiroyuki TAKANO[1)], Takahide KOHRO[2)], Kazutaka UEDA[1)], Yuriko NIITSUMA[1)], Hiroyuki ABURATANI[2)], and Issei KOMURO[1)]

Although recent clinical studies have suggested that long-acting calcium channel blockers (CCBs) have beneficial effects on heart failure, the precise mechanism is unknown. In this study, Dahl salt-sensitive rats fed a high salt diet were treated with the long-acting CCB amlodipine, the low–molecular-weight membrane permeable superoxide dismutase mimetic 4-hydroxy-2,2,6,6-tetramethyl piperidinoxyl (Tempol), or saline from 11 weeks after birth. The cardiac geometry and function, and gene expression profiles were determined at 17 weeks. Dahl salt-sensitive rats fed a high salt diet followed by saline as a non-treatment control (HS group) showed a marked increase in blood pressure and developed concentric hypertrophy at 11 weeks, followed by left ventricular (LV) dilation and congestive heart failure by 17 weeks. The treatment with amlodipine (AMLO group) or Tempol (TEMP group) significantly inhibited the development of LV hypertrophy and cardiac dysfunction. Analysis using an Affymetrix GeneChip U34 revealed that the expression levels of 195 genes were changed by the treatment with amlodipine. Among these 195 genes, 110 genes were increased in HS rats and decreased in AMLO rats. And of these 110 genes, 54 genes were also decreased in TEMP rats. In contrast, 85 genes were decreased in HS rats and increased in AMLO rats. Of these 85 genes, 38 genes were also increased in TEMP rats. Approximately 48% of the genes were changed in similar fashion in AMLO and TEMP rats, suggesting that amlodipine shows beneficial effects on heart failure mainly *via* antioxidative mechanisms. (*Hypertens Res* 2006; 29: 719–729)

***Key Words*: amlodipine, Dahl rat, gene chip, heart failure, hypertension**

Introduction

Hemodynamic overload, which can take the form of pressure or volume overload, causes left ventricular (LV) hypertrophy as an adaptive mechanism. However, sustained cardiac hypertrophy induces a reduction of contractile ability and/or a decrease in the number of viable myocytes, resulting in congestive heart failure (CHF) (*1–4*). It is very important to elucidate the molecular mechanism of the progression from cardiac hypertrophy to heart failure (*5*).

Calcium channel blockers (CCBs) are widely used to treat patients with hypertension (*6*), but treatment with short-acting CCBs has been reported to increase the risk of cardiovascular death, at least partly due to activation of the sympathetic nervous system (*7–9*). However, CCBs with an intrinsically long duration of activity have been shown to significantly reduce vascular resistance properties without significant effects on myocardial contractility (*10*). In the ACTION (A Coronary disease Trial Investigating Outcome with Nifedipine GITS [gastro-intestinal therapeutic system]) trial, the addition of long-acting nifedipine to conventional treatment of stable

From the [1)]Department of Cardiovascular Science and Medicine, Chiba University Graduate School of Medicine, Chiba, Japan; and [2)]Genome Science Division, Research Center for Advanced Science and Technology, University of Tokyo, Tokyo, Japan.

This work was supported by Health and Labour Sciences Research Grants, by a Grant-in-Aid from the Japan Medical Association, and by the Takeda Medical Research Foundation, the Uehara Memorial Foundation, the Kato Memorial Trust for Nambyo Research, and the Takeda Science Foundation.

Address for Reprints: Issei Komuro, M.D., Ph.D., Department of Cardiovascular Science and Medicine, Chiba University Graduate School of Medicine (M4), 1–8–1 Inohana, Chuo-ku, Chiba 260–8670, Japan. E-mail: komuro-tky@umin.ac.jp

Received January 24, 2006; Accepted in revised form May 29, 2006.

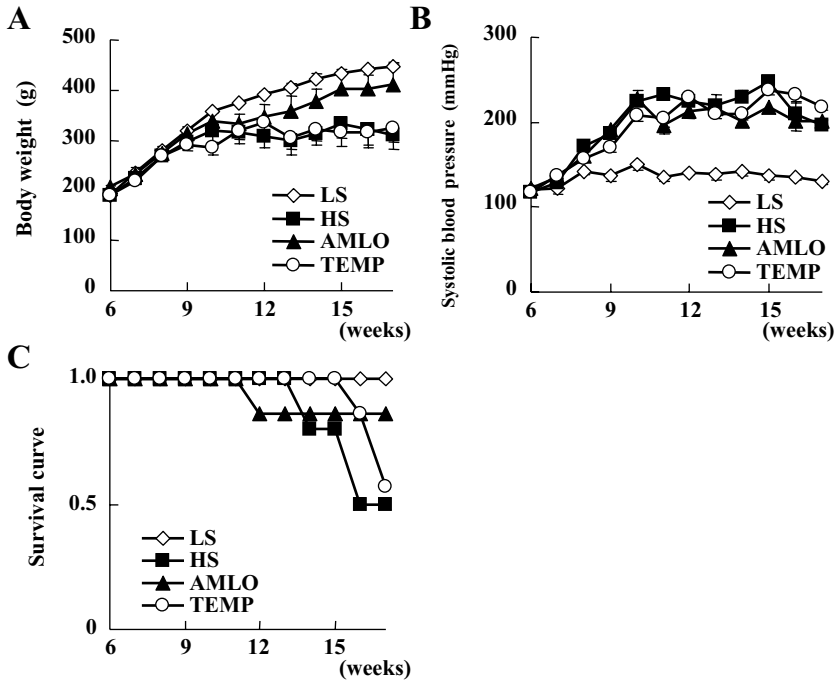

Fig. 1. *The change of blood pressure, body weight and mortality. A: The time course of body weight in LS, HS, AMLO and TEMP rats. Data are expressed as the mean±SEM (*n*=10, 10, 7, 7, respectively). B: The time course of systolic blood pressure (SBP) in LS, HS and AMLO rats. Data are expressed as the mean±SEM (*n*=10, 10, 7, 7, respectively). C: The time course of survival rate in LS, HS and AMLO rats (*n*=10, 10, 7, 7, respectively).*

angina patients reduced the development of heart failure by 29% (*11*, *12*).

Amlodipine, a third generation dihydropyridine CCB, has much higher affinity for lipid constituents of the cellular membrane than do other CCBs (*13*). There are increasing basic and clinical data indicating that amlodipine and other CCBs, in addition to having hemodynamic properties, exert non–calcium channel-related pleiotropic actions, such as the release of nitric oxide (*14*), inhibition of adhesion molecules (*15*) and inhibition of matrix metalloproteinase-1 (*16*). Moreover, amlodipine inhibits cytokine-induced endothelial cell toxicity and has a potent membrane antioxidant activity independent of its calcium channel modulation (*17*). To determine whether amlodipine prevents the progression from hypertrophy to heart failure, we used a Dahl rat hypertensive heart failure model (*18–22*), and to gain insight into the underlying mechanisms of the effects of amlodipine, we performed DNA chip analysis (*23*, *24*).

Methods

Animals

Five-week-old male Dahl salt-sensitive rats (DS) were obtained from SLC (Shizuoka, Japan). All rats were housed in climate-controlled metabolic cages with a 12:12-h light-dark cycle. Twenty-four rats were fed a diet containing 0.3% NaCl until the age of 6 weeks, then fed a diet containing 8% NaCl (MF; Oriental Yeast, Tokyo, Japan) from 6 weeks of age until the end of the experiment. Seven of these 24 rats were then given amlodipine (10 mg/kg/day) by gavage once a day from 11 weeks to 17 weeks (AMLO group), 7 were given the low–molecular-weight membrane permeable superoxide dismutase (SOD) mimetic, 4-hydroxy-2,2,6,6-tetramethyl piperidinoxyl (Tempol; 10 mg/kg/day), by gavage once a day from 11 weeks to 17 weeks (TEMP group) and 10 rats were treated with saline as a non-treatment control (HS group). In addition, 10 rats were fed a diet containing 0.3% NaCl throughout this experiment as a normal blood pressure control (LS group). The blood pressure (BP) and body weight (BW) of all animals were measured every week. The peak systolic pressure was recorded by a photoelectric pulse device (Softron BP-98A; Softron Co., Tokyo, Japan) placed on the tail of unanesthetized rats as described previously (*25*). At 17 weeks of age, all DS rats with or without CHF were sacrificed, before their natural death, when signs of CHF such as rapid and labored respiration and LV diffuse hypokinesis on echocardiography were observed.

Throughout the studies, all animals were treated humanely in accordance with the guidelines on animal experimentation of our institute and the Position of the American Heart Association on Research Animal Use. All protocols were approved

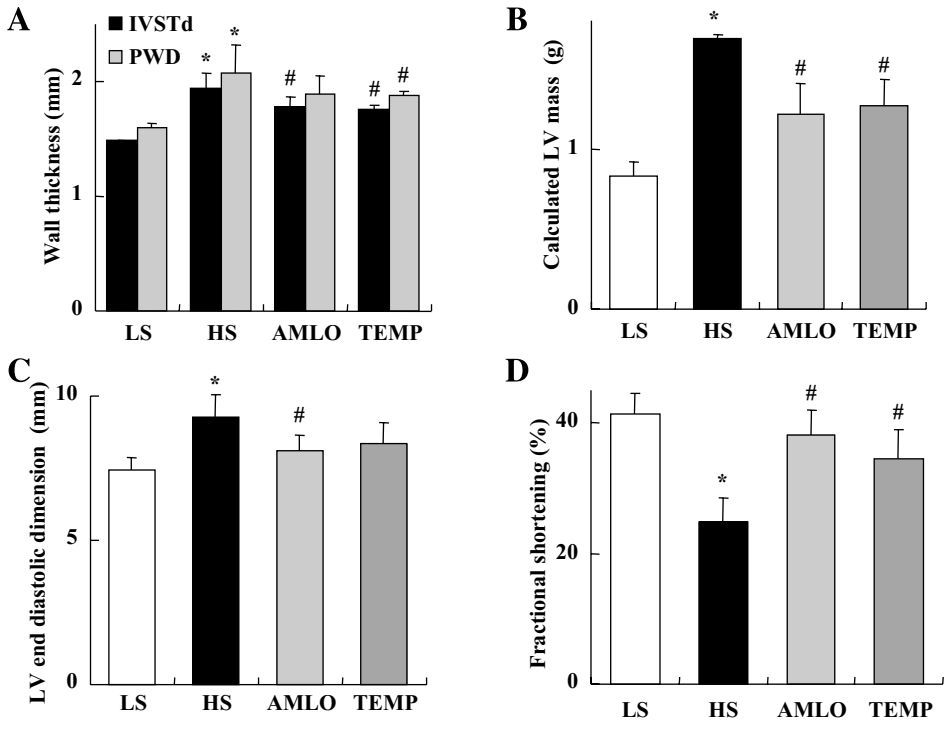

Fig. 2. *The results of echocardiography of DS rats at 17 weeks. A: The wall thickness of IVSTd and PWTd of LV of LS, HS, AMLO and TEMP rats at 17 weeks (*n = *10, 5, 6, 4, respectively). B: The calculated LV mass of LS, HS, AMLO and TEMP rats at 17 weeks (*n = *10, 5, 6, 4, respectively). C: The LVDd of LS, HS, AMLO and TEMP rats at 17 weeks (*n = *10, 5, 6, 4, respectively). D: The fractional shortening of LS, HS, AMLO and TEMP rats at 17 weeks (*n = *10, 5, 6, 4, respectively). Data are expressed as the mean ± SEM.* *$p < 0.05$ vs. *LS rats.* #$p < 0.05$ vs. *HS rats.*

by the Institutional Animal Care and Use Committee of Chiba University Graduate School of Medicine.

Echocardiography

The LV dimension, contraction, LV wall thickness, and LV fractional shortening (FS) were determined by echocardiography after anesthesia with an intramuscular injection of pentobarbital sodium (15 mg/kg BW). Transthoracic echocardiography was performed at the ages of 6, 11, and 17 weeks in all rats using an HP Sonos 5500 (Hewlett-Packard Co., Andover, USA) with a 10-MHz imaging linear scan probe transducer as described previously (*25*, *26*).

Histological Analysis

The heart was weighed, then fixed by perfusion with 3.8% formaldehyde, embedded in paraffin, sectioned into 4 μm slices, and stained with hematoxylin-eosin (H-E) or van Gieson stain (*25*). To determine the degree of collagen fiber accumulation, we selected 10 fields at random and calculated the ratio of the fibrotic area by van Gieson staining to the total myocardial area by using NIH IMAGE software (NIH Research Service Branch, Bethesda, USA) (*25*). Apoptosis was detected by *in situ* terminal deoxynucleotidyl transfer-mediated end labeling of fragmented nuclei (TUNEL assay) using an *in situ* apoptosis detection kit (CardioTACS™; TREVIGEN Inc., Gaithersburg, USA) according to the supplier's instructions. The oxidation of the myocardium was determined by immunostaining using anti–4-hydroxy-2-nonenal antibody (anti-4-HNE; ALEXIS Biochemicals, USA) reacted with avidin-conjugated peroxidase (VECTASTAIN ABC kit, VECTOR, Burlingame, USA), and visualized with 3,3′-diaminobenzidine (Peroxidase substrate kit DAB, VECTOR). For semiquantification, the area and the intensity of 4-HNE staining were scored as reported previously (*27*). A part of the LV was frozen at −80°C for mRNA analysis.

RNA Preparation and DNA Microarray Analysis

Total RNA was isolated from rat heart ventricles using the lithium/urea method and separated on a 1.0% agarose/formaldehyde gel. cDNA of brain natriuretic peptide (BNP) was labeled by a random priming method with [α-^{32}P]dCTP and hybridized to membranes as described previously (*25*). An RNase protection assay (using 20 μg of total RNA) was performed using a rat cytokine Multi-Probe Template Set (BD Pharmingen Bioscience, San Jose, USA) according to the

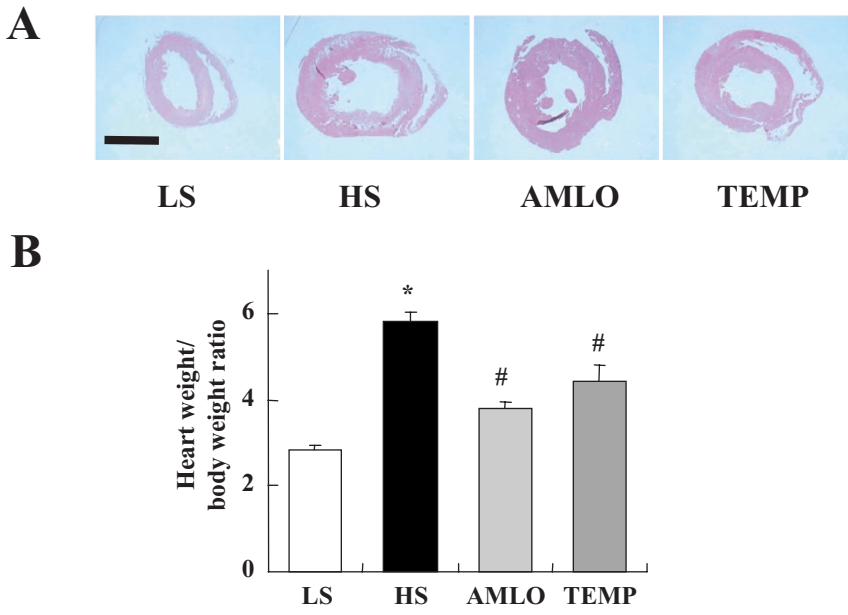

Fig. 3. *The heart-weight-to-body-weight ratio of DS rats at 17 weeks. A: H-E staining of the heart of LS, HS, AMLO and TEMP rats at 17 weeks (*n = *10, 5, 6, 4, respectively). The bar indicates 5 mm. B: The heart-weight-to-body-weight ratio of LS, HS, AMLO and TEMP rats at 17 weeks (*n = *10, 5, 6, 4, respectively). Data are expressed as the mean ± SEM.* *p < *0.05* vs. *LS rats.* #p < *0.05* vs. *HS rats.*

manufacturer's instructions (*25*). Hybridized bands were quantified with a FUJIX Bio-Imaging Analyzer BAS 2000 (Fuji Film Co., Tokyo, Japan). Polyadenylate [poly(A)+] RNA was purified from the total RNA with a QuickPrep mRNA purification kit (Pharmacia Biotech, Piscataway, USA). The experimental procedures for the gene chip analysis were performed according to the Affymetrix GeneChip Expression Analysis Technical Manual (Affymetrix, Santa Clara, USA) (*28–30*). The Affymetrix GeneChip U34A set was derived from selected genes and ESTs from the 18 November 1998 release of Genbank. Each 8800 gene is represented on the arrays by perfectly matched 25-mer (PM) oligonucleotides and mismatched (MM) 25-mer control probes that are identical except for one base. The expression levels were calculated by background-subtracting the hybridization signal of MM from its PM partner and averaging the difference for the probe pair set for individual genes. The RNA levels of each gene were scanned and scored for which the computer algorithm (Affymetrix) returned a "present" call. All calculations were performed by Affymetrix software (*31*). The data were analyzed by the program FileMaker Pro 4.0 for Macintosh. Among the 8,800 clones included in the gene chip analysis, we selected those genes having an intensity of >100. Among these genes, we picked out ratio values >1.7 or <−1.7 as indicating genes with changed expression.

Statistical Analysis

All data are expressed as the mean±SEM of 3–4 independent experiments. Mean differences among the 4 groups were tested by one-way ANOVA followed by Scheffe's modified *F*-test for multiple comparisons. Comparisons of follow-up body weight, blood pressure, pulse rate and echocardiographic data were tested using repeated measure ANOVA followed by Scheffe's modified *F*-test. Values of $p<0.05$ were considered statistically significant.

Results

Development of Cardiac Hypertrophy and Heart Failure in Dahl Salt-Sensitive Rats

A loss of body weight was observed in HS rats, but the treatment with amlodipine significantly attenuated it (Fig. 1A). The initial systolic BP (SBP) at 6 weeks of age was 108.5±11.4 mmHg (mean±SEM, $n=34$). SBP was gradually increased, reached a level of over 200 mmHg by 11 weeks, and remained over 200 mmHg thereafter in HS rats. The SBP was not decreased in AMLO or TEMP rats and there was no significant difference in SBP among HS, AMLO and TEMP rats (Fig. 1B). At the age of 14–16 weeks, all HS rats lost BW and displayed rapid and labored respiration characteristic of CHF, and by 17 weeks, 5 of 10 rats had died. On the other hand, all LS rats were alive without any symptoms and 6 of 7

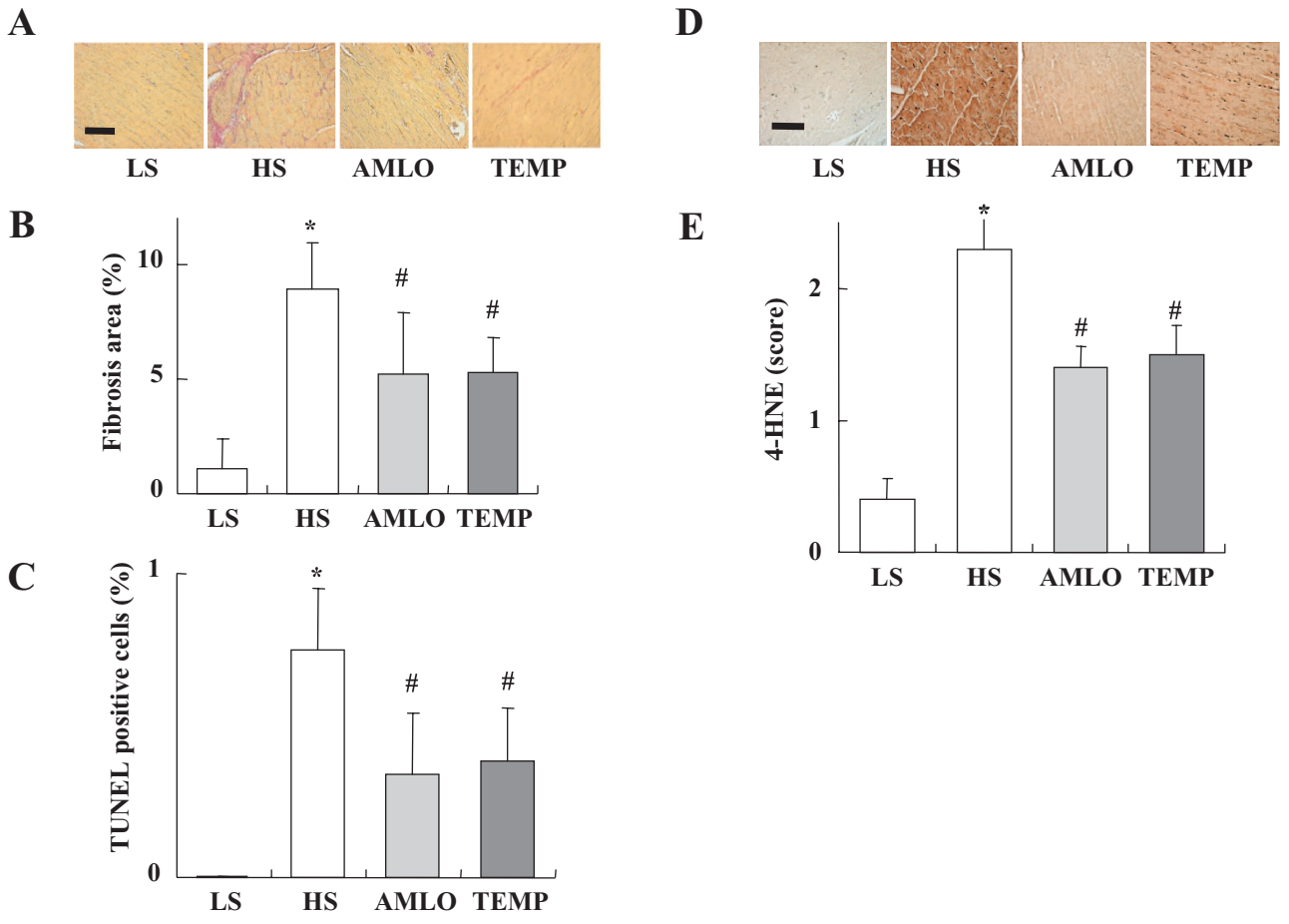

Fig. 4. *The fibrosis and apoptosis of DS rats. A: Representative photographs of von Gieson staining of the heart of LS, HS, AMLO and TEMP rats at 17 weeks. The bar indicates 100 μm. B: The percentage of fibrotic area in the heart of LS, HS, AMLO and TEMP rats at 17 weeks (*n = *10, 5, 6, 4, respectively). C: The percentage of TUNEL-positive cells in the heart of LS, HS, AMLO and TEMP rats at 17 weeks (*n = *10, 5, 6, 4, respectively). D: Representative photographs of 4-HNE staining of the heart of LS, HS, AMLO and TEMP rats at 17 weeks. The bar indicates 100 μm. E: The scoring of the staining of 4-HNE of the heart of LS, HS, AMLO and TEMP rats at 17 weeks (*n = *10, 5, 6, 4, respectively). Data are expressed as the mean ± SEM.* $^{*}p < 0.05$ vs. *LS rats.* $^{\#}p < 0.05$ vs. *HS rats.*

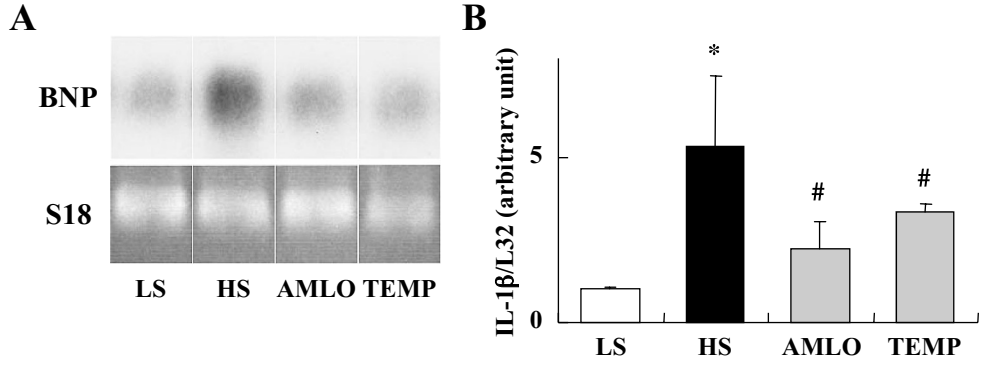

Fig. 5. *The gene expression of DS rats. A: Representative photograph of the expression of BNP using Northern blot analysis. B: The expression of IL-1β of LS, HS, AMLO and TEMP rats at 17 weeks determined by RNase protection assay. Data are expressed as the mean ± SEM.* $^{*}p < 0.05$ vs. *LS rats.* $^{\#}p < 0.05$ vs. *HS rats.*

Table 1. The List of Genes Increased in HS and Decreased in AMLO and TEMP Rats Heart

	HS/LS	AMLO/HS	TEMP/HS	Accession No.
Cell division				
Rat mRNA for cdc25B, complete cds	2.9	−4.6	−1.8	D16237
Cyclin D1	1.8	−2.3	−2.1	D14014
Cell signaling				
Arachidonate 12-lipoxygenase	217.9	−231.6	−226.8	L06040
Pancreatitis-associated protein	51.3	−17.7	−3.3	M98049
Cell adhesion molecule, neural (CD56)	18.3	−12.4	−5.4	AI137246
Neuron specific protein PEP-19 (Purkinje cell protein 4)	14.8	−14.3	−13.9	M24852
Lysyl oxidase	13.3	−8.9	−6.4	S66184
Arg/Abl-interacting protein ArgBP2	10.6	−2.9	−2.0	AI058393
Rattus norvegicus mRNA Best5 protein	10.2	−3.6	−4.6	Y07704
Fibronectin (cell-, heparin-, and fibrin-binding domains) gene	8.1	−2.1	−1.7	L00191
Carbonic anhydrase II gene	8.1	−7.7	−6.8	U60578
Sialoprotein (osteopontin)	7.0	−3.7	−2.0	M14656
Rattus norvegicus mRNA Best5 protein	6.6	−2.9	−3.8	Y07704
Rattus norvegicus protein kinase C-binding protein Enigma mRNA	5.3	−4.7	−2.9	U48247
Isk protein	5.0	−6.0	−2.7	D10709
Prostaglandin F2α receptor	5.0	−3.3	−1.7	S74898
GATA-binding protein 4	5.0	−2.7	−2.1	L22761
Calcium channel, voltage-dependent, T type, α1G subunit	4.0	−4.1	−2.0	AF027984
Transforming growth factor-β stimulated clone 22	3.9	−3.4	−1.8	L25785
Follistatin-related protein precursor	3.7	−2.4	−1.8	AA849769
Taurine/β-alanine transporter	3.6	−2.7	−2.0	M96601
S100 Ca-binding protein A4	3.6	−3.2	−2.1	X06916
N^G,N^G-Dimethylarginine dimethylaminohydrolase	3.6	−3.1	−2.4	AA894273
Lipocortin V	3.3	−2.4	−2.2	AF051895
Vesicle-associated membrane protein 5	3.0	−2.5	−1.7	AF054826
Solute carrier family 4, member 1, anion exchange protein 1 (kidney band 3)	2.8	−2.7	−2.8	AA866414
Cadherin 2, type 1, *N*-cadherin (neuronal)	2.7	−2.1	−1.7	AF097593
Muscle Y-box protein YB2	2.7	−2.9	−2.2	D28557
Cerebellar Ca-binding protein, spot 35 protein	2.5	−2.6	−2.2	M31178
Rhesus blood group	2.3	−2.4	−1.8	AB015191
Galectin-5	2.3	−3.3	−2.2	L21711
Immediate-early serum-responsive JE gene	2.2	−1.7	−1.8	X17053
Enolase 1, α	2.1	−1.9	−1.7	X02610
Prolyl endopeptidase	2.1	−5.5	−2.4	AB012759
Glutathione-S-transferase, mu type 2 (Yb2)	2.0	−1.7	−2.1	J02810
Cyclic protein-2=cathepsin L proenzyme	2.0	−2.5	−2.8	S85184
ASM15	2.0	−2.3	−1.8	X59864
Glycogenin	2.0	−1.9	−1.7	U96130
Rat VL30 element mRNA	1.9	−2.2	−1.7	M91234
Adenylyl cyclase–associated protein 2	1.8	−2.0	−1.8	AI145367
Ezrin	1.8	−1.8	−1.7	X67788
Cell structure				
Fast myosin alkali light chain	9.5	−8.0	−2.1	L00088
Rattus norvegicus α-globin (GloA) gene, complete cds	4.9	−7.5	−2.5	AI178971
Ribosomal protein L3	2.7	−2.1	−1.7	X62166
Transthyretin (prealbumin, amyloidosis type I)	2.4	−2.3	−2.2	AA945169
Metabolism				
Aminolevulinate synthase 2, δ	6.7	−9.5	−3.7	D86297
Phosphofructokinase C	4.9	−3.2	−2.0	L25387
Ornithine decarboxylase antizyme inhibitor	2.8	−1.7	−1.8	AI043631

Table 1. (Continued)

	HS/LS	AMLO/HS	TEMP/HS	Accession No.
Unclassified				
ESTs				
ESTs, highly similar to G0S2 MOUSE PUTATIVE LYMPHOCYTE G0/G1 SWITCH PROTEIN 2	22.2	−2.4	−5.2	AA893235
ESTs	16.9	−16.4	−2.4	AA894092
ESTs, weakly similar to T14355 protein-tyrosine-phosphatase [R. norvegicus]	5.4	−6.7	−2.1	AA800303
ESTs, highly similar to 60S RIBOSOMAL PROTEIN L3 [R. norvegicus]	3.8	−2.7	−1.8	AA892367
ESTs	2.5	−3.4	−2.9	AA944361
ESTs	1.9	−2.4	−2.8	H31625

HS/LS, the fold change the gene expression of HS to LS rat; AMLO/HS, the fold change the gene expression of AMLO to HS rat; TEMP/HS, the fold change the gene expression of TEMP to HS.

AMLO rats and 4 of 7 TEMP rats were alive at 17 weeks (Fig. 1C).

Echocardiography

We assessed cardiac geometry and function by echocardiography. In accordance with the increase of SBP, LV wall thickness was increased in HS rats at 17 weeks compared to LS rats (Fig. 2A). The diastolic interventricular septum wall thickness (IVSTd) was significantly thinner in AMLO and TEMP rats than in HS rats (Fig. 2A). The calculated LV mass was increased in HS rats, and treatment with either amlodipine or Tempol reduced it (Fig. 2B). In parallel with the progression of the symptoms of heart failure, LV was dilated (Fig. 2C) and the contraction was impaired (Fig. 2D) in HS rats compared with LS rats. The treatment with either amlodipine or Tempol significantly attenuated the development of LV hypertrophy and dilatation, and improved contraction (Fig. 2A–D).

Histopathology of the Heart

HS rats developed remarkable cardiac hypertrophy compared with LS rats (the weights of the hearts of 17-week-old animals were as follows: LS, 1.25±0.02 mg; HS, 1.84±0.09 mg; AMLO, 1.56±0.12 mg; TEMP, 1.48±0.09 mg; HS *vs*. AMLO, $p<0.05$; HS *vs*. TEMP, $p<0.05$). The heart-weight-to-body-weight (H/B) ratios of the 17-week-old animals were as follows: LS, 2.82±0.14; HS, 5.82±0.20 ($p<0.05$) (Fig. 3). The increase in the H/B ratio was attenuated significantly in the AMLO group and TEMP group compared with the HS group (AMLO, 3.78±0.16, $p<0.05$ *vs*. HS; TEMP, 4.42±0.40, $p<0.05$ *vs*. HS) (Fig. 3). Marked cardiomyocyte hypertrophy and interstitial fibrosis were observed in the LV tissue of 17-week-old HS rats compared to LS rats (Fig. 4A). Quantitative analysis of myocardial fibrosis using van Gieson staining of the heart tissue revealed that the treatment with either amlodipine or Tempol significantly reduced the fibrotic area compared to that in HS rats (LS, 1.1±1.3%; HS, 8.9±3.9%; AMLO, 5.2±2.7%; TEMP, 5.3±1.5%; HS *vs*. AMLO, $p<0.05$; HS *vs*. TEMP, $p<0.05$) (Fig. 4B). Apoptosis has been reported to be involved in the pathophysiology of the development of heart failure in DS rats (*32*). The number of apoptotic cells was increased in HS rats compared to LS rats, but the treatment with either amlodipine or Tempol significantly reduced the number of apoptotic cells detected by the TUNEL method (Fig. 4C). Since the staining score of 4-HNE (a by-product of lipid peroxidation and an indicator of oxidative stress) of the myocardium was increased in HS hearts compared to LS hearts, it was improved in AMLO and TEMP hearts (Fig. 4D, E).

Effects of Amlodipine Treatment on Gene Expression

The mRNA levels of brain natriuretic peptide (BNP) and interleukin (IL)-1β were significantly higher in HS rats compared to LS rats, as reported previously (*33*), indicating that this model of hypertensive heart failure was reliable. The treatment with either amlodipine or Tempol significantly reduced the expression levels of BNP (Fig. 5A) and IL-1β (Fig. 5B) genes. Other myocardial gene expression profiling results were obtained from the gene chip analysis of RNA samples from the hearts of each group. Upregulations of the natriuretic peptide factor precursor A (ANF), BNP, c-fos, β-myosin heavy chain (β-MHC) and Egr-1 genes (data not shown), all of which are known to be upregulated in CHF, were detected by the gene chip, suggesting the reliability of the RNA expression analysis. Since both amlodipine and Tempol significantly inhibited the transition of LV hypertrophy to heart failure, we compared the gene expression profile of each heart treated with either amlodipine or Tempol using a gene chip. Amlodipine treatment changed the expression of 195 genes, and some of these genes may be involved in the beneficial effects of amlodipine on heart failure. Among these 195 genes, 110 genes were increased in HS rats and decreased in AMLO rats. And of these 110 genes, 54 genes were also decreased in TEMP rats (Table 1). Eighty-five genes were

Table 2. The List of Genes Decreased in HS and Increased in AMLO and TEMP Rats Heart

	HS/LS	AMLO/HS	TEMP/HS	Accession No.
Cell signaling				
Aquaporin 7	−42.9	31.7	12.4	AB000507
D site albumin promoter binding protein	−28.4	4.6	17.8	J03179
Mitogen activated protein kinase kinase 2	−12.5	12.2	4.8	L14936
ATPase, Na^+K^+ transporting, α2 polypeptide	−7.2	5.0	4.1	AI177026
Retinoid X receptor γ	−6.2	4.7	2.4	AF016387
A-raf	−5.7	3.1	2.0	X06942
Putative G protein–coupled receptor (SENR) gene	−5.5	6.5	4.2	AB012210
Protein tyrosine phosphatase, non-receptor type 16	−4.9	2.6	2.2	U02553
MHC class II gene	−4.3	3.8	3.5	D45240
Ras-related rab1B protein	−4.1	3.5	3.6	X13905
Pyruvate dehydrogenase kinase, isoenzyme 4	−4.1	4.4	2.8	AF034577
ORF mRNA	−4.0	5.3	4.5	L41685
Guanidinoacetate methyltransferase	−3.9	3.2	1.8	X08056
Dynorphin gene	−3.5	4.4	5.0	M32783
Glycerol-3-phosphate acyltransferase	−3.3	4.2	1.9	U36773
Cytochrome b5	−3.1	2.1	3.3	AA945054
CD74 antigen	−2.7	2.7	2.4	X13044
α-2-Macroglobulin gene exon 1	−2.6	2.6	2.8	X13983
Rat mRNA for pulmonary surfactant-associated protein SP-B	−2.5	2.5	1.8	AI170380
Vitronectin	−2.5	2.2	1.7	U44845
Short chain acyl-coenzyme A dehydrogenase	−2.4	1.9	1.7	J05030
Secretin receptor	−2.2	2.0	1.7	X59132
Short isoform growth hormone receptor	−2.1	2.4	2.0	S49003
Small heterodimer partner homologue	−1.9	1.7	2.0	D86745
Olfactory neuron-specific (clone 50.06, promoter)	−1.9	1.8	1.9	S64924
Ptk-3L=radiation-induced gene	−1.9	1.9	2.3	S77585
Rat mRNA for MHC class II antigen RT1.B-1 β-chain	−1.7	1.8	2.3	X56596
Cell structure				
Myosin, heavy polypeptide 9, non-muscle	−3.0	3.9	2.9	U31463
Metabolism				
Carboxylesterase 1	−5.6	7.0	5.0	L46791
Rattus norvegicus serine protease gene, complete cds	−2.1	2.0	2.0	L38482
Unclassified				
ESTs				
ESTs, weakly similar to T17307 hypothetical protein DKFZp566O084.1	−16.8	13.3	6.6	AI639268
ESTs, highly similar to JN0873 immunophilin p59-mouse	−12.5	12.6	7.3	AI136977
ESTs, highly similar to NUIM_HUMAN NADH-UBIQUINONE OXIDOREDUCTASE 23 kD SUBUNIT PRECURSOR	−4.8	3.8	2.8	AA799479
ESTs, moderately similar to 60S RIBOSOMAL PROTEIN L3	−3.6	3.0	2.1	AA891037
ESTs	−3.4	3.5	2.3	AI009098
ESTs, weakly similar to T13607 hypothetical protein EG:87B1.3-fruit fly	−2.8	2.1	1.7	AI639504
ESTs, highly similar to ROA2 MOUSE HETEROGENEOUS NUCLEAR RIBONUCLEOPROTEINS A2/B1	−2.6	2.5	1.7	AA799511
ESTs	−2.1	1.8	1.9	AA800298

HS/LS, the fold change the gene expression of HS to LS rat; AMLO/HS, the fold change the gene expression of AMLO to HS rat; TEMP/HS, the fold change the gene expression of TEMP to HS.

decreased in HS rats and increased in AMLO rats. Of these 85 genes, 38 genes were also increased in TEMP rats (Table 2). The genes that changed in a similar fashion in both AMLO and TEMP rats may have been involved in the antioxidative mechanisms of amlodipine on hypertensive heart failure. Fibrosis-related genes (arachidonate 12-lipoxygenase, trans-

forming growth factor-β and fibronectin) and proinflammatory/proapoptotic genes (pancreatitis-associated protein, lysyl oxidase, sialoprotein, prostaglandin F2α receptor, galectin-5, enolase 1) were included among the 54 genes that were increased in HS rats but decreased in AMLO and TEMP rat. Several Ca-handling protein genes, such as voltage-dependent protein, T type protein, α1G subunit protein, S100 Ca-binding protein A4, cerebellar Ca-binding protein, and spot 35 protein genes were also included. By contrast, several genes, *i.e.*, aquaporin 9, CD74, vitronectin, mitogen-activated protein kinase kinase (MAPKK) and A-raf, were upregulated by the treatment with either amlodipine or Tempol.

Discussion

In the present study, we demonstrated the beneficial effects of the long-term CCB amlodipine on hypertensive heart failure. Treatment with amlodipine significantly reduced the heart weight, LV wall thickness and LV diameter, and improved LV systolic function. Increases in expression levels of the BNP and IL-1β gene were inhibited by the treatment with amlodipine. Moreover, we investigated the changes in the expression levels of a large number of genes in the hearts of LS, HS, AMLO and TEMP rats at the heart failure stage.

In this study, we used Tempol as an antioxidative drug. Tempol is a low–molecular-weight super oxide dismutase mimetic that is both metal-independent and cell membrane permeable. Several investigators have suggested that Tempol reduces O_2-induced damage during inflammation, radiation, and ischemic/reperfusion injury. Although Tempol improved the cardiac function and hypertrophy in our study, the mortality and the BW loss were not improved. This chemical compound may cause some systemic adverse effects. Since the inhibitory effect of Tempol on the hypertrophied heart is controversial, the mechanisms of the induction of the hypertrophy such as hypoxia (*34*), isoproterenol (*35*) or aldosterone (*36*) may be related to the difference.

Many factors, such as the renin-angiotensin system (*37*), calcineurin (*26*, *38*), the endothelin-system (*33*, *39*), and IL-1β (*33*), have been reported to be involved in the transition from compensated cardiac hypertrophy to decompensated heart failure in DS rats. They also include abnormalities in calcium handling, apoptosis of cardiac myocytes, increases in cytokine expression and extracellular matrix, and activation of neurohumoral factors. The DS rat develops systemic hypertension, depending on the amount of sodium supplied in the diet, and cardiac hypertrophy with interstitial fibrosis. Prolonged hypertension induces reduced myocardial contraction and relaxation velocities (*19*, *20*), indicating that this model fully recapitulates the phenotype of human LV hypertrophy and hypertensive heart failure.

Treatment with short-acting CCBs may worsen heart failure and increase the risk of death in patients with advanced LV dysfunction. Amlodipine can regulate membrane fluidity and cholesterol deposition, stimulate NO production to recruit its biologic actions, and regulate matrix deposition. Recognition of the ancillary actions of amlodipine is important for understanding the agent's mechanisms of action and the pathologic mechanisms underlying cardiovascular disease. The antioxidant properties of amlodipine are attributed to its chemical structure and direct physicochemical interactions with the membrane lipid bilayer, as evidenced by changes in membrane thermodynamic properties (*40*). Oxidative stress is widely known to play important roles in the pathophysiology of hypertensive heart failure. In the present study, treatment with amlodipine improved the degree of cardiac hypertrophy, dilatation, contraction and mortality. The improvement of cardiac fibrosis and a decrease in apoptosis may be involved in the mechanism of the beneficial effects of amlodipine. Although it is difficult to analyze the pathophysiological mechanism by which amlodipine inhibits the progression of heart failure, our finding that the drug altered the expression levels of various genes may provide a clue.

An antioxidative mechanism may be involved in the beneficial effects of amlodipine in heart failure. Amlodipine has been reported to inhibit oxidative stress in the hypertensive hypertrophied heart (*41*). By the treatment with amlodipine, 195 genes were changed and these genes may be involved in the beneficial effects of amlodipine on heart failure. Among these 195 genes, 110 genes were increased in HS rats and decreased in AMLO rats. In 110 genes, 54 genes were also decreased in TEMP rats. These genes that were changed in a similar fashion in AMLO and TEMP rats may be involved in the antioxidative mechanisms of amlodipine on hypertensive heart failure. Many of these genes have been classified as cell signaling–related genes. Since fibrosis-related genes such as arachidonate 12-lipoxygenase (*42*), transforming growth factor-β and fibronectin are known to be involved in the pathophysiology of cardiac fibrosis, they were changed similarly by the treatment with either amlodipine or Tempol. Proinflammatory and/or proapoptotic genes such as pancreatitis-associated protein, lysyl oxidase, sialoprotein, prostaglandin F2α receptor, galectin-5 and enolase 1 are also included in this group. Pancreatitis-associated protein is reported to be related to play a role in inflammatory pancreatitis (*43*). Lysyl oxidase is an enzyme involved in extracellular matrix maturation (*44*). Prostaglandin F2α is reported to have the ability to oxidize arachidonate. Galectin is a β-galactoside–binding protein that is related to the initiation of apoptosis. Enolase 1 is reported to be involved in the aging of neural cells (*45*). The role of these proteins in the failing heart is unknown, and further investigations will be needed. Since Ca-handling proteins have not previously been reported to be involved in the mechanism of CCB on the heart, several Ca-handling protein genes, such as the voltage-dependent, T type, α1G subunit, S100 Ca-binding protein A4, cerebellar Ca-binding protein, and spot 35 protein genes, are also included in this group. Further study is needed to clarify the effect of these genes.

In contrary, in 195 genes, 85 genes were decreased in HS rats and increased in AMLO rats. In 85 genes, 38 genes were

also increased in TEMP rats. These genes may be involved in the protective effects on heart failure. Some of these genes such as aquaporin 9, which is mostly changed, were not known as cardiovascular-related genes. Since macrophage migration inhibitory factor (MIF) is reported to delay the progression of apoptosis (*46*), CD74, which is known as an MIF-binding protein (*47*), may have important roles in the protective mechanism of amlodipine. Since the activation of coagulation is involved in the pathophysiology of heart failure, vitronectin, which is a co-factor along with plasminogen activator inhibitor 1 (*48*) for the inhibition of thrombin, is upregulated. Other changed genes may also have important roles in the beneficial mechanisms of amlodipine on the heart. A novel mechanism of amlodipine on the development of heart failure may become obvious by use of our result.

In conclusion, the present study demonstrated that the long-term CCB amlodipine has beneficial effects on a hypertensive heart failure model. A genome-wide study using a gene chip provided various clues that should be useful for determining the beneficial antioxidative mechanisms of amlodipine on hypertensive heart failure.

Acknowledgements

We thank Reiko Kobayashi, Emi Fujita, Megumi Ikeda, Akane Furuyama, and Yuko Ohtsuki for their technical assistance.

References

1. Levy D, Garrison RJ, Savage DD, *et al*: Prognostic implications of echocardiographically determined left ventricular mass in the Framingham Heart Study. *N Engl J Med* 1990; **322**: 1561–1566.
2. Frohlich ED: Cardiac hypertrophy in hypertension. *N Engl J Med* 1987; **317**: 831–833.
3. Katz AM: The cardiomyopathy of overload: an unnatural growth response in the hypertrophied heart. *Ann Intern Med* 1994; **121**: 363–371.
4. Tavi P, Laine M, Weckstrom M, *et al*: Cardiac mechanotransduction: from sensing to disease and treatment. *Trends Pharmacol Sci* 2001; **22**: 254–260.
5. Komuro I: Molecular mechanism of cardiac hypertrophy and development. *Jpn Circ J* 2001; **65**: 353–358.
6. Chobanian AV, Bakris GL, Black HR, *et al*, National Heart, Lung, and Blood Institute Joint National Committee on Prevention, Detection, Evaluation, and Treatment of High Blood Pressure; National High Blood Pressure Education Program Coordinating Committee: The Seventh Report of the Joint National Committee on Prevention, Detection, Evaluation, and Treatment of High Blood Pressure: the JNC 7 report. *JAMA* 2003; **289**: 2560–2572.
7. Wilcox RG, Hampton JR, Banks DC, *et al*: Trial of early nifedipine in acute myocardial infarction: the Trent study. *Br Med J* 1986; **293**: 1204–1208.
8. The Israeli Sprint Study Group: Secondary prevention reinfarction Israeli nifedipine trial (SPRINT). A randomized intervention trial of nifedipine in patients with acute myocardial infarction. *Eur Heart J* 1988; **9**: 354–364.
9. Furberg CD, Psaty BM, Meyer JV: Nifedipine. Dose-related increase in mortality in patients with coronary heart disease. *Circulation* 1995; **92**: 1326–1331.
10. Spinale FG, Mukherjee R, Krombach RS, *et al*: Chronic amlodipine treatment during the development of heart failure. *Circulation* 1998; **98**: 1666–1674.
11. Lubsen J, Wagener G, Kirwan BA, *et al*: Effect of long-acting nifedipine on mortality and cardiovascular morbidity in patients with symptomatic stable angina and hypertension: the ACTION trial. *J Hypertens* 2005; **23**: 641–648.
12. Poole-Wilson PA, Lubsen J, Kirwan BA, *et al*: Effect of long-acting nifedipine on mortality and cardiovascular morbidity in patients with stable angina requiring treatment (ACTION trial): randomised controlled trial. *Lancet* 2004; **364**: 849–857.
13. Mason RP, Campbell SF, Wang SD, Herbette LG: Comparison of location and binding for the positively charged 1,4-dihydropyridine calcium channel antagonist amlodipine with uncharged drugs of this class in cardiac membranes. *Mol Pharmacol* 1989; **36**: 634–640.
14. Zhang X, Hintze TH: Amlodipine releases nitric oxide from canine coronary microvessels: an unexpected mechanism of action of a calcium channel–blocking agent. *Circulation* 1998; **97**: 576–580.
15. Cominacini L, Pasini AF, Pastorino AM, *et al*: Comparative effects of different dihydropyridines on the expression of adhesion molecules induced by TNF-alpha on endothelial cells. *J Hypertens* 1999; **17**: 1837–1841.
16. Ikeda U, Hojo Y, Ueno S, Arakawa H, Shimada K: Amlodipine inhibits expression of matrix metalloproteinase-1 and its inhibitor in human vascular endothelial cells. *J Cardiovasc Pharmacol* 2000; **35**: 887–890.
17. Mason RP, Marche P, Hintze TH: Novel vascular biology of third-generation L-type calcium channel antagonists: ancillary actions of amlodipine. *Arterioscler Thromb Vasc Biol* 2003; **23**: 2155–2163.
18. Rapp JP, Wang SM, Dene H: A genetic polymorphism in the renin gene of Dahl rats cosegregates with blood pressure. *Science* 1989; **243**: 542–544.
19. Inoko M, Kihara Y, Morii I, *et al*: Transition from compensatory hypertrophy to dilated, failing left ventricles in Dahl salt-sensitive rats. *Am J Physiol* 1994; **267**: H2471–H2482.
20. Inoko M, Kihara Y, Sasayama S: Neurohumoral factors during transition from left ventricular hypertrophy to failure in Dahl salt-sensitive rats. *Biochem Biophys Res Commun* 1995; **206**: 814–820.
21. Iwanaga Y, Kihara Y, Hasegawa K, *et al*: Cardiac endothelin-1 plays a critical role in the functional deterioration of left ventricles during the transition from compensatory hypertrophy to congestive heart failure in salt-sensitive hypertensive rats. *Circulation* 1998; **98**: 2065–2073.
22. Nishikawa N, Masuyama T, Yamamoto K, *et al*: Long-term administration of amlodipine prevents decompensation to diastolic heart failure in hypertensive rats. *J Am Coll Cardiol* 2001; **38**: 1539–1545.
23. Duggan DJ, Bittner M, Chen Y, Meltzer P, Trent JM: Expression profiling using cDNA microarrays. *Nat Genet* 1999; **21**: 10–14.
24. Shiffman D, Porter JG: Gene expression profiling of cardio-

vascular disease models. *Curr Opin Biotechnol* 2000; **11**: 598–601.
25. Hasegawa H, Yamamoto R, Takano H, *et al*: 3-Hydroxy-3-methylglutaryl coenzyme A reductase inhibitors prevent the development of cardiac hypertrophy and heart failure in rats. *J Mol Cell Cardiol* 2003; **35**: 953–960.
26. Shimoyama M, Hayashi D, Zou Y, *et al*: Calcineurin inhibitor attenuates the development and induces the regression of cardiac hypertrophy in rats with salt-sensitive hypertension. *Circulation* 2000; **102**: 1996–2004.
27. Liu YH, Carretero OA, Cingolani OH, *et al*: Role of inducible nitric oxide synthase in cardiac function and remodeling in mice with heart failure due to myocardial infarction. *Am J Physiol Heart Circ Physiol* 2005; **289**: H2616–H2623.
28. Ishii M, Hashimoto S, Tsutsumi S, *et al*: Direct comparison of GeneChip and SAGE on the quantitative accuracy in transcript profiling analysis. *Genomics* 2000; **68**: 136–143.
29. Lockhart DJ, Dong H, Byrne MC, *et al*: Expression monitoring by hybridization to high-density oligonucleotide arrays. *Nat Biotechnol* 1996; **14**: 1675–1680.
30. Lee CK, Klopp RG, Weindruch R, *et al*: Gene expression profile of aging and its retardation by caloric restriction. *Science* 1999; **285**: 1390–1393.
31. Mizukami M, Hasegawa H, Kohro T, *et al*: Gene expression profile revealed different effects of angiotensin II receptor blockade and angiotensin-converting enzyme inhibitor on heart failure. *J Cardiovasc Pharmacol* 2003; **42**: S1–S6.
32. Ikeda S, Hamada M, Qu P, *et al*: Relationship between cardiomyocyte cell death and cardiac function during hypertensive cardiac remodelling in Dahl rats. *Clin Sci* 2002; **102**: 329–335.
33. Shioi T, Matsumori A, Kihara Y, *et al*: Increased expression of interleukin-1 beta and monocyte chemotactic and activating factor/monocyte chemoattractant protein-1 in the hypertrophied and failing heart with pressure overload. *Circ Res* 1997; **81**: 664–671.
34. Elmedal B, de Dam MY, Mulvany MJ, *et al*: The superoxide dismutase mimetic, tempol, blunts right ventricular hypertrophy in chronic hypoxic rats. *Br J Pharmacol* 2004; **141**: 105–113.
35. Zhang GX, Kimura S, Nishiyama A, *et al*: Cardiac oxidative stress in acute and chronic isoproterenol-infused rats. *Cardiovasc Res* 2005; **65**: 230–238.
36. Yoshida K, Kim-Mitsuyama S, Wake R, *et al*: Excess aldosterone under normal salt diet induces cardiac hypertrophy and infiltration *via* oxidative stress. *Hypertens Res* 2005; **28**: 447–455.
37. Yamamoto K, Masuyama T, Sakata Y, *et al*: Roles of renin-angiotensin and endothelin systems in development of diastolic heart failure in hypertensive hearts. *Cardiovasc Res* 2000; **47**: 274–283.
38. Hayashida W, Kihara Y, Yasaka A, Sasayama S: Cardiac calcineurin during transition from hypertrophy to heart failure in rats. *Biochem Biophys Res Commun* 2000; **273**: 347–351.
39. Iwanaga Y, Kihara Y, Inagaki K, *et al*: Differential effects of angiotensin II *versus* endothelin-1 inhibitions in hypertrophic left ventricular myocardium during transition to heart failure. *Circulation* 2001; **104**: 606–612.
40. Mason RP, Walter MF, Trumbore MW, Olmstead EG Jr, Mason PE: Membrane antioxidant effects of the charged dihydropyridine calcium antagonist amlodipine. *J Mol Cell Cardiol* 1999; **31**: 275–281.
41. Umemoto S, Tanaka M, Kawahara S, *et al*: Calcium antagonist reduces oxidative stress by upregulating Cu/Zn superoxide dismutase in stroke-prone spontaneously hypertensive rats. *Hypertens Res* 2004; **27**: 877–885.
42. Wen Y, Gu J, Peng X, Zhang G, Nadler J: Overexpression of 12-lipoxygenase and cardiac fibroblast hypertrophy. *Trends Cardiovasc Med* 2003; **13**: 129–136.
43. Niederau C, Schonberg M: New developments in the pathophysiology of inflammatory pancreatic disease. *Hepatogastroenterology* 1999; **46**: 2722.
44. Raposo B, Rodriguez C, Martinez-Gonzalez J, Badimon L: High levels of homocysteine inhibit lysyl oxidase (LOX) and downregulate LOX expression in vascular endothelial cells. *Atherosclerosis* 2004; **177**: 1–8.
45. Poon HF, Vaishnav RA, Butterfield DA, *et al*: Proteomic identification of differentially expressed proteins in the aging murine olfactory system and transcriptional analysis of the associated genes. *J Neurochem* 2005; **94**: 380–392.
46. Baumann R, Casaulta C, Simon D, Conus S, Yousefi S, Simon HU: Macrophage migration inhibitory factor delays apoptosis in neutrophils by inhibiting the mitochondria-dependent death pathway. *FASEB J* 2003; **17**: 2221–2230.
47. Leng L, Metz CN, Fang Y, *et al*: MIF signal transduction initiated by binding to CD74. *J Exp Med* 2003; **197**: 1467–1476.
48. Xiang G, Schuster MD, Seki T, *et al*: Down-regulation of plasminogen activator inhibitor 1 expression promotes myocardial neovascularization by bone marrow progenitors. *J Exp Med* 2004; **200**: 1657–1666.